Preparation and Properties of Diruthenium Hydrido Complexes Having a Bridging Benzoquinone Ligand: Formation of an Alcohol Adduct of a μ-η^2:η^2-Benzoquinone Complex through Hydrogen Bonding

Toshiro Takao, Kazunori Akiyoshi, and Hiroharu Suzuki*

Department of Applied Chemistry, Graduate School of Science and Engineering, Tokyo Institute of Technology, 2-12-1 O-okayama, Meguro-ku, Tokyo 152-8552, Japan

Received April 24, 2008

Diruthenium hydrido complexes containing a bridging 1,4-benzoquinone ligand, {Cp*Ru(μ-H)}$_2$(μ-η^2:η^2-$C_6H_3RO_2$) (**2a**, R = H; **2b**, R = Me, Cp* = η^5-C_5Me_5), were synthesized by the reaction of a diruthenium tetrahydrido complex, Cp*Ru(μ-H)$_4$RuCp* (**1**), with 1,4-benzoquinone and 2-methyl-1,4-benzoquinone. Spectroscopic data unambiguously indicated that the hydrogen bond between the quinonoid oxygen atoms of **2** and alcohol molecules changed the electronic nature of the metal center such that it was significantly different from that in aprotic solvent. Therefore, the rate of the reaction of **2a** with acetylene, which afforded a μ-η^2-vinyl-μ-η^2:η^2-benzoquinone complex, (Cp*Ru)$_2$(μ-H)(μ-η^2-CH=CH$_2$)(μ-η^2:η^2-$C_6H_4O_2$) (**3**), in methanol was 3 times the rate of reaction in benzene.

Introduction

We have studied skeletal rearrangement of hydrocarbyl ligands on a triruthenium plane induced by chemical oxidation,[1] and we showed that a trimetallic complex having a μ_3-η^3-C_3 ring was formed by the 2e oxidation of a μ_3-diruthenaallyl complex via reductive C−C bond formation.[1a,c] Oxidation led to the reduction in electron density at the metal center, which was compensated by a change in the coordination mode of the hydrocarbyl ligand.[2] In contrast, a weak interaction on an ancillary ligand, such as a hydrogen bond, is expected to affect the electronic nature of the metal center. In this context, a π-bonded 1,4-benzoquinone ligand would be promising for controlling the electronic environment of the metal center because a π-bonded quinone ligand is still able to interact with proton or Lewis acid through oxygen atoms, and the electronic perturbation occurring at the oxygen atom could be transferred to the metal center through its π-conjugation.

Several complexes containing a 1,4-quinone π-bonded to a transition metal have been synthesized thus far,[3–5] and the interconversion among η^4-quinone, η^5-semiquinone, and η^6-dihydroquinone complexes associated with proton and electron transfer from the metal center has been elucidated.[6] Recently, Sweigart and co-workers demonstrated that an anionic rhodium complex containing a 1,4-quinone ligand catalyzes the arylation of aldehydes with arylboronic acid, and they proposed the importance of the interaction between the quinonoid oxygen atom and boron in the reaction.[7] Such weak acid−base interaction at the supporting ligand could lead to a substantial electronic influence on the metal center as well as on its reactivity; however, little information is available on the influence of such weak interactions on the metal center.

In this article, we describe the synthesis and properties of novel diruthenium complexes having a bridging 1,4-quinone ligand as a junction of a hydrogen bond. Unlike other complexes containing a quinonoid molecule, these complexes contain a hydrido ligand, which initiates further reaction on the metal center. This enables us to examine the influence of the hydrogen bond held at the quinonoid ligand on reactivity; further, it is observed that a significant acceleration of the reaction of a μ-benzoquinone complex, {Cp*Ru(μ-H)}$_2$(μ-$C_6H_4O_2$) (**2a**, Cp* = η^5-C_5Me_5), with acetylene resulted in the formation of a μ-vinyl-μ-benzoquinone complex.

* Corresponding author. E-mail: hiroharu@n.cc.titech.ac.jp.

(1) (a) Takao, T.; Inagaki, A.; Murotani, E.; Imamura, T.; Suzuki, H. *Organometallics* **2003**, *22*, 1361–1363. (b) Takao, T.; Inagaki, A.; Imamura, T.; Suzuki, H. *Organometallics* **2006**, *25*, 5511–5514. (c) Takao, T.; Moriya, M.; Suzuki, H. *Organometallics* **2007**, *26*, 1349–1360.

(2) Geiger, W. E. *Organometallics* **2007**, *26*, 5738–5765.

(3) Foster, R.; Foreman, M. I. In *The Chemistry of the Quinonoid Compounds*; Patai, S., Eds.; John Wiley & Sons: New York, 1974; Part 1, Chapter *6*, pp 257−333.

(4) See, for example: (a) Sternberg, H. W.; Markby, R.; Wender, I. *J. Am. Chem. Soc.* **1958**, *80*, 1009–1010. (b) Schrauzer, G. N.; Thyret, H. *J. Am. Chem. Soc.* **1960**, *82*, 6420–6421. (c) Schrauzer, G. N.; Thyret, H. *Angew. Chem., Int. Ed. Engl.* **1963**, *2*, 478. (d) Davidson, J. L.; Green, M.; Stone, F. G. A.; Welch, A. J. *J. Chem. Soc., Dalton Trans.* **1976**, 738–745. (e) Fairhurst, G.; White, C. *J. Chem. Soc., Dalton Trans.* **1979**, 1531–1538. (f) Jewell, C. F., Jr.; Liebeskind, L. S.; Williamson, M. *J. Am. Chem. Soc.* **1985**, *107*, 6715–6716. (g) Ura, Y.; Sato, Y.; Shiotsuki, M.; Suzuki, T.; Wada, K.; Kondo, T.; Mitsudo, T. *Organometallics* **2003**, *22*, 77–82.

(5) (a) Masaoka, S.; Tanaka, D.; Nakanishi, Y.; Kitagawa, S. *Angew. Chem., Int. Ed.* **2004**, *43*, 2530–2534. (b) Masaoka, S.; Akiyama, G.; Horike, S.; Kitagawa, S.; Ida, T.; Endo, K. *J. Am. Chem. Soc.* **2003**, *125*, 1152–1153. (c) Yamamoto, Y.; Ohno, T.; Itoh, K. *Organometallics* **2003**, *22*, 267–2272. (d) Klein, R. A.; Witte, P.; van Belzen, R.; Fraanje, J.; Goubitz, K.; Numan, M.; Schenk, H.; Ernsting, J. M.; Elsevier, C. J. *Eur. J. Inorg. Chem.* **1998**, 319–330.

(6) (a) Sun, S.; Carpenter, G. B.; Sweigart, D. A. *J. Organomet. Chem.* **1996**, *512*, 257–259. (b) Oh, M.; Carpenter, G. B.; Sweigart, D. A. *Organometallics* **2002**, *21*, 1290–1295. (c) Huang, Y.-S.; Sabo-Etienne, S.; He, X.-D.; Chaudret, B.; Boubekeur, K.; Batall, P. *Organometallics* **1992**, *11*, 3031–3035. (d) Bras, J. L.; Amouri, H.; Vaissermann, J. *J. Organomet. Chem.* **1998**, *553*, 483–485. (e) Bras, J. L.; Amouri, H.; Vaissermann, J. *Organometallics* **1998**, *17*, 1116–1121.

(7) (a) Son, S. U.; Kim, S. B.; Reingold, J. A.; Carpenter, G. B.; Sweigart, D. A. *J. Am. Chem. Soc.* **2005**, *127*, 12238–12239. (b) Trenkle, W. C.; Barkin, J. L.; Son, S. U.; Sweigart, D. A. *Organometallics* **2006**, *25*, 3548–3551.

(8) (a) Suzuki, H.; Omori, H.; Lee, D. H.; Yoshida, Y.; Moro-oka, Y. *Organometallics* **1988**, *7*, 2579–2581. (b) Suzuki, H.; Omori, H.; Lee, D. H.; Yoshida, Y.; Fukushima, M.; Tanaka, M.; Moro-oka, Y. *Organometallics* **1994**, *13*, 1129–1146. (c) Suzuki, H. *Eur. J. Inorg. Chem.* **2002**, 1009–1023.

10.1021/om800363f CCC: $40.75
Publication on Web 07/29/2008

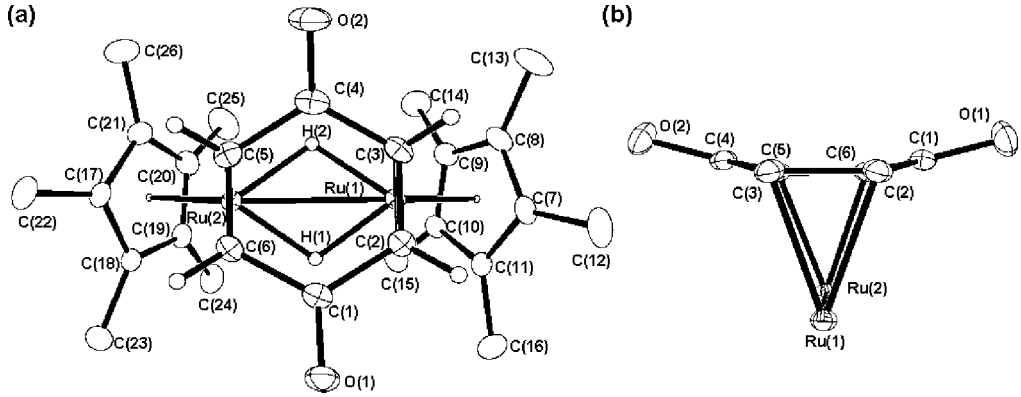

Figure 1. Molecular structure and labeling scheme of **2a** with thermal ellipsoids at the 30% probability level: (a) top view; (b) side view of the core of **2a** along with the Ru(1)−Ru(2) axis.

Table 1. Selected Bond Lengths (Å) and Angles (deg) of 2a

Ru(1)−Ru(2)	2.7367(2)	Ru(1)−C(2)	2.1685(17)	Ru(1)−C(3)	2.1664(17)
Ru(2)−C(5)	2.1614(18)	Ru(2)−C(6)	2.1860(17)	C(1)−O(1)	1.235(2)
C(1)−C(2)	1.474(2)	C(1)−C(6)	1.468(3)	C(2)−C(3)	1.428(2)
C(3)−C(4)	1.464(3)	C(4)−O(2)	1.234(2)	C(4)−C(5)	1.474(3)
C(5)−C(6)	1.433(2)				
C(2)−Ru(1)−C(3)	38.47(7)			C(5)−Ru(2)−C(6)	38.48(7)
O(1)−C(1)−C(2)	120.58(17)			O(1)−C(1)−C(6)	122.68(17)
C(2)−C(1)−C(6)	116.71(15)			C(1)−C(2)−C(3)	120.86(17)
C(2)−C(3)−C(4)	120.84(16)			O(2)−C(4)−C(3)	122.08(18)
O(2)−C(4)−C(5)	121.55(19)			C(3)−C(4)−C(5)	116.33(15)
C(4)−C(5)−C(6)	121.41(17)			C(1)−C(6)−C(5)	119.96(16)

Result and Discussion

The treatment of a diruthenium tetrahydrido complex, Cp*Ru(μ-H)$_4$RuCp* (**1**, Cp* = η^5-C_5Me_5),[8] with 1,4-quinone resulted in the exclusive formation of a μ-benzoquinone complex, {Cp*Ru(μ-H)}$_2$(μ-η^2:η^2-$C_6H_4O_2$) (**2a**), with a yield of 94% (eq 1).

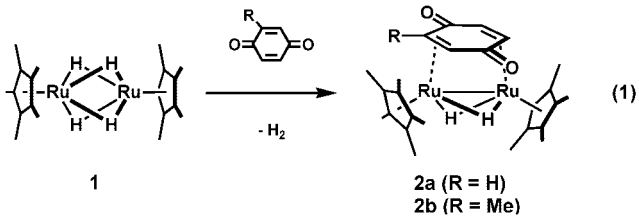

(1)

Although there were a few reports on the preparation of a bimetallic complex containing a μ-η^2:η^2-1,4-quinone ligand,[5] to the best of our knowledge, this is the first example of a μ-η^2:η^2-1,4-quinone complex possessing a hydrido ligand.[9]

In the ^{1}H NMR spectrum of **2a** in benzene-d_6 solution, the signal derived from the hydrido ligands were observed at δ −16.26 as a singlet. The four methine protons of the bridging benzoquinone ligand were also observed to be equivalent at δ 5.27. The symmetrical structure of **2a** was corroborated by means of an X-ray diffraction study carried out using a dark green single crystal obtained from a THF/pentane solution (Figure 1). The relevant bond lengths and angles are listed in Table 1.

The ORTEP diagram clearly shows that the 1,4-quione ligand bridges two ruthenium nuclei in a *syn*-μ-η^2:η^2-fashion. The two ruthenium nuclei were separated from each other by a distance of 2.7367(2) Å. This value is slightly shorter than the Ru−Ru bond distance expected for a Ru−Ru single bond (2.75−2.93 Å)[10] and significantly longer than the Ru−Ru bond distance of **1** (2.4630(5) Å).[8b] The reduction in the Ru−Ru distance of **2a** is explained by electronic reasons: according to the 18-electron rule applied to **2a**, a double bond must be formed between the two ruthenium atoms due to its 32-electron configuration.

The π-coordinated C═C bond distances of **2a** (C(2)−C(3) = 1.428(2) Å, C(5)−C(6) = 1.433(2) Å) are considerably longer than the C═C bond distance of the uncoordinated 1,4-benzoquinone (1.334 Å)[11] and slightly longer than the values reported for the μ-η^2:η^2-benzoquinone complexes (1.351−1.425 Å).[5] This elongation implies the strong back-donation from the electron-rich [Cp*Ru] fragment. The μ-benzoquinone ligand adopts a boat-like conformation like other η^4-coordinated quinone complexes (Figure 1b), and the torsion angle C(1)−C(2)−C(6)−C(3) was −167.4°. The C═O bond distances (C(1)−O(1) = 1.235(2) Å, C(4)−O(2) = 1.234(2) Å) lie in the upper limit of the reported range for the μ-η^2:η^2-benzoquinone complexes (1.213−1.236 Å).[5]

Kitagawa and co-workers reported coordination networks based on Cu_2(μ-η^2:η^2-C_6H_4O)(μ-$OCOCH_3$)$_2$ as an organometallic building block.[5a] An X-ray diffraction study has shown that the networks are formed by the intermolecular interaction between the metal center and the lone pairs of the quinonoid oxygen atoms, in addition to the intramolecular π-coordination of the diene moiety to the bimetallic center. Due to the bulky

(9) There were also a few examples of the monometallic π-bonded quinone complex containing a hydrido ligand: (a) Rosete, R. O.; Cole-Hamilton, D. J.; Wilkinson, G. *J. Chem. Soc., Dalton Trans.* **1979**, 1618–1623. (b) Schrauzer, G. N.; Dewhirst, K. C. *J. Am. Chem. Soc.* **1964**, *86*, 3265–3270.

(10) (a) Nucciarone, D.; Taylor, N. J.; Carty, A. J.; Tripicchio, A.; Camellini, M. A.; Sappa, E. *Organometallics* **1988**, *7*, 118–126. (b) Churchill, M. R.; Hollander, F. J.; Hutchinson, J. P. *Inorg. Chem.* **1977**, *16*, 2655–2659.

(11) van Bolhuis, F.; Kiers, C. T. *Acta Crystallogr.* **1978**, *B34*, 1015–1016.

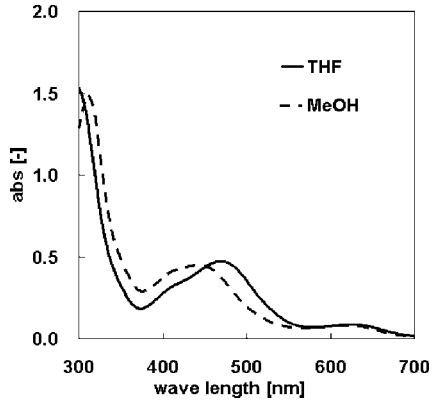

Figure 2. UV−vis spectra of 0.1 mM **2a** in THF (—) and MeOH (---) at 25 °C.

Cp* groups, such an intermolecular interaction would be suppressed in the crystal of **2a**.

In the ^{1}H NMR spectra of **2b**, which were obtained by the reaction of **1** with 2-methyl-1,4-benzoquinone, two Cp* signals were found to be inequivalent due to the presence of a methyl group on the quinone ligand (δ 1.32_6 and 1.33_3). The signals stemming from the hydrido ligands were also observed to be inequivalent at δ −16.88 and −16.22 (J_{H-H} = 4.4 Hz). The hydrido ligand of **2** was nonfluxional within the NMR time scale, and the shapes of these signals did not change up to 80 °C.

While the color of the solution of **2a** in THF was light brown, it turns olive-green in methanol (see the Supporting Information). In the UV−vis spectrum measured in THF, two peaks were observed at 625 (ε_{max} = 907 M^{-1} cm^{-1}) and 470 nm (ε_{max} = 4901 M^{-1} cm^{-1}) (Figure 2). From these peaks, only the peak derived from the MLCT transition (470 nm) underwent a hypsochromic shift to 443 nm (ε_{max} = 4649 M^{-1} cm^{-1}) in methanol. This solvatochromism strongly suggests the interaction of **2** with alcohol, possibly the presence of a hydrogen bond between the oxygen atom of the quinone ligand and a proton. A similar hypsochromic shift was observed in the UV−vis spectra of the π-coordinated duroquinone complex (η^5-C_5H_5)Co(η^4-$C_6Me_4O_2$) measured in perchloric acid solution.[9b]

The relationship between the magnitude of the hypsochromic shift and the acidity of alcohol used as solvent was found; the peak indicating the maximum of the MLCT absorption appeared at 453 nm in 2-propanol (pK_a = 16.5), whereas it was found at 404 nm in hexafluoro-2-propanol (pK_a = 9.4). In addition, the incorporation of deuterium into the hydrido position of **2a** did not occur in methanol-d_4 solution at least within 200 h at ambient temperature. The lack of H/D exchange strongly suggests that the proton was not coordinated on the metal center, but the carbonyl group.

When phenol is used, an alcohol adduct of **2a** was successfully isolated as a single crystal (eq 2). A dark red single crystal of the phenol adduct, **2a-PhOH**, was obtained by the slow diffusion of pentane into a THF solution of **2a** in the presence of 30 equiv of phenol at room temperature. The structure of **2a-PhOH** is shown in Figure 3, and relevant bond lengths and angles are listed in Table 2.

In a unit cell, 2.5 molecules of phenol were present and all of them were bound to the oxygen atom of the quinone ligand through their phenolic protons. O···O distances between the quinone ligand and the phenol ranged from 2.63 to 2.75 Å, which were comparable to the O···O distance of 2.74 Å

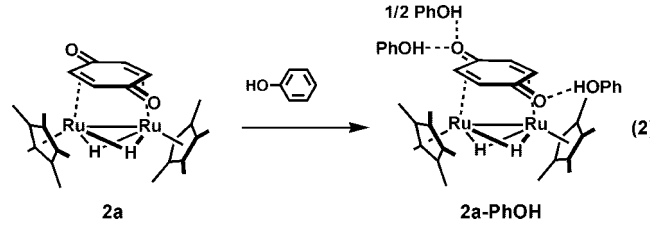

reported for quinhydrone, in which quinone and hydroquinone were connected via hydrogen bonding.[12]

Although the change in the bond distances around the quinone moiety between those of parent **2a** was rather small (within 0.02 Å), the dihedral angles of the quinone moiety increased significantly. The benzoquinone moiety became flat due to the presence of a hydrogen bond; the torsion angle C(1)−C(2)−C(6)−C(3) changed from −167.4° in **2a** to −173.10° in **2a-PhOH**. These changes were possibly due to the contribution of a dihydroquinone structure, and this requires electron transfer from the metal centers to the benzoquinone ligand, i.e., a stronger back-donation.

The hydrogen bond also caused a considerable decrease in the bond order of the carbonyl group. In the IR spectrum, a sharp absorption attributable to ν(CO) of **2a** was observed at 1619 cm^{-1}, whereas this absorption shifted toward lower frequency in **2a-PhOH** (1568 cm^{-1}).

The hydrogen bond affects the redox potential of the metal center of **2a**, which was observed in a cyclic voltammogram. The quinone/hydroquinone redox couple has been frequently used in numerous biological processes[13] and in organic synthesis;[14] however, to date, the electrochemistry of related complexes such as π-bonded 1,4-quinone complexes has hardly been studied.[15]

In the THF solution, two quasi-reversible redox waves were observed within the potential window (Figure 4). The redox wave found at $E_{1/2}$ = −1.92 V (vs ferrocene) was attributed to the formation of a one-electron-reduced anionic species, and that observed at $E_{1/2}$ = −43 mV is assignable to the formation of a one-electron-oxidized cationic species.[16] Since the redox couple attributable to the formation of an anionic species was not observed for the parent tetrahydrido complex **1** within the potential window of THF, the redox process at $E_{1/2}$ = −1.92 V was probably assignable to the reduction of the benzoquinone ligand. Under the same experimental conditions, THF solutions of free 1,4-benzoquinone exhibit a reduction wave at $E_{1/2}$ = −1.06 V. On complexation, the redox potential shifted toward the negative values, as observed for other η^4-1,4-quinone complexes.[15]

(12) Sakurai, T. *Acta Crystallogr.* **1968**, *B24*, 403–412.

(13) Bentley, R.; Campbell, I. M. In *The Chemistry of the Quinonoid Compounds*; Patai, S., Eds.; John Wiley & Sons: New York, 1974; Part 2, Chapter 13, pp 683−736.

(14) (a) Becker, H.-D. In *The Chemistry of the Quinonoid Compounds*; Patai, S., Eds.; John Wiley & Sons: New York, 1974; Part 1, Chapter 7, pp 335−423. (b) Fu, P. P.; Harvey, R. G. *Chem. Rev.* **1978**, *78*, 317–361.

(15) (a) Moussa, J.; Guyard-Duhayon, C.; Herson, P.; Amouri, H.; Rager, M. N.; Jutand, A. *Organometallics* **2004**, *23*, 6231–6238. (b) Hiramatsu, M.; Shiozaki, K.; Fujinami, T.; Sakai, S. *J. Organomet. Chem.* **1983**, *246*, 203–211. (c) Hiramatsu, M.; Nakano, H.; Fujinami, T.; Sakai, S. *J. Organomet. Chem.* **1982**, *236*, 131–138.

(16) The values of the limiting current of both redox processes were obtained by means of rotating disk electrode measurements using the Koutecky−Levich equation, and each process was assigned to be a one-electron process by comparison with the current of ferrocene. A green precipitate, which was assignable to the one-electron-oxidized species, was prepared by the chemical oxidation of **2a** using ferrocenium salt. Isolation as well as structural determination is currently underway.

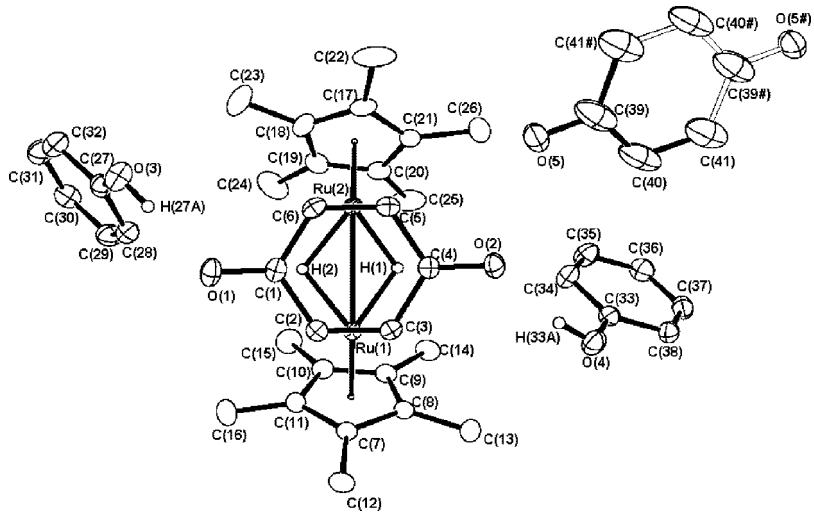

Figure 3. Molecular structure and labeling scheme of **2a-PhOH** with thermal ellipsoids at the 30% probability level.

Table 2. Selected Bond Lengths (Å) and Angles (deg) of 2a-PhOH

Ru(1)−Ru(2)	2.74011(16)	Ru(1)−C(2)	2.1638(13)	Ru(1)−C(3)	2.1749(13)
Ru(2)−C(5)	2.1676(15)	Ru(2)−C(6)	2.1747(14)	C(1)−O(1)	1.2466(19)
C(1)−C(2)	1.459(2)	C(1)−C(6)	1.457(2)	C(2)−C(3)	1.421(2)
C(3)−C(4)	1.458(2)	C(4)−O(2)	1.2463(18)	C(4)−C(5)	1.460(2)
C(5)−C(6)	1.422(2)	O(1)···O(3)	2.638(2)	O(2)···O(4)	2.680(2)
O(2)···O(4)	2.746(3)	O(1)−H(27A)	1.86(3)	O(1)−H(33A)	1.89(3)
C(2)−Ru(1)−C(3)	38.25(5)			C(5)−Ru(2)−C(6)	38.23(6)
O(1)−C(1)−C(2)	120.55(15)			O(1)−C(1)−C(6)	122.43(14)
C(2)−C(1)−C(6)	116.96(13)			C(1)−C(2)−C(3)	121.87(13)
C(2)−C(3)−C(4)	120.66(13)			O(2)−C(4)−C(3)	121.94(14)
O(2)−C(4)−C(5)	120.82(14)			C(3)−C(4)−C(5)	117.18(13)
C(4)−C(5)−C(6)	121.61(14)			C(1)−C(6)−C(5)	120.92(14)

The most prominent feature of the electrochemical behavior of **2a** is the reversibility of both the redox processes. The cyclic voltammogram is considerably different from that of the monometallic η^4-1,4-quinone complexes, which showed irreversible redox waves.[15] During the electrochemical studies of the monometallic η^4-1,4-quinone complexes, the formation of free benzoquinone is also detected. Thus, the reversibility found in **2a** is likely to originate from the difference in the coordination mode of the 1,4-benzoquinone ligand in **2a**; the binding of the μ-η^2:η^2-coordinated benzoquinone ligand to the two metal nuclei is stronger than that in the monometallic system.

As for free benzoquinone, Smith and co-workers elucidated the role of the hydrogen-bonded quinone dianion in unbuffered aqueous solution, which highly stabilizes the dianionic form and facilitates the reduction of the quinone anion to the dianion effectively.[17] Since the redox potential shifted toward the negative values on complexation, we cannot detect the influence of the hydrogen bonding in the reduced form. However, the influence on the metal center caused by the hydrogen bonding was clearly seen.

In methanol, only one oxidation peak was observed due to the narrow potential window of the solvent. Further, the redox potential considerably shifts toward the positive direction ($E_{1/2}$ = 147 mV). The magnitude of the positive shift showed good correlation with the pK_a value of the solvent. The redox potential was 275 mV in trifluoroethanol (pK_a = 12.5), whereas it was 34 mV in 2-propanol (pK_a = 16.5). These facts strongly indicate that the hydrogen bond between the benzoquinone ligand and the alcohol lowers the energy level of the HOMO of **2**.

The hydrogen bond at the oxygen atom of the benzoquinone ligand would lower the energy level of the π*(C═C) bond through π-conjugation. This leads to a strong interaction between the metal center and the benzoquinone moiety and makes a large contribution of the dihydroquinone structure as seen in **2a-PhOH**. Due to the electron transfer from the metal center to the quinone moiety, the electron density at the metal center would be reduced considerably, and this probably causes the stabilization of the HOMO. Therefore, the hypsochromic shift observed in the methanol solution may be rationalized by the stabilization of the HOMO of **2a** owing to the presence of a hydrogen bond.

Since the electron density at the metal center of **2a** was reduced in protic media due to the presence of the hydrogen bond through the 1,4-quinone ligand, the reactivity should be significantly affected. Thus, we examined the reactions of **2a** with acetylene in benzene and methanol. The reactions proceeded in a similar manner to yield a μ-vinyl-μ-η^2:η^2-1,4-benzoquinone complex, (Cp*Ru)$_2$(μ-η^2:η^2-C$_6$H$_4$O$_2$)(μ-H)(μ-η^2-CH═CH$_2$) (**3**), but the reaction rate accelerated significantly in methanol (eq 3).

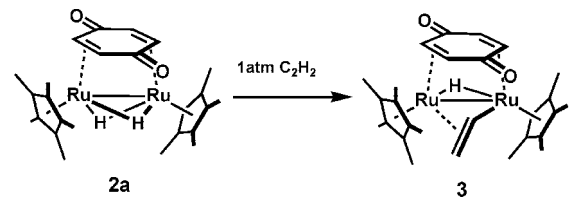

The reaction of **2a** with 1 atm of acetylene was monitored by means of ^{1}H NMR spectroscopy. In both benzene and methanol, the reaction proceeded selectively, but the reaction

(17) Quan, M.; Sanchez, D.; Wasylkiw, M. F.; Smith, D. K. *J. Am. Chem. Soc.* **2007**, *129*, 12847–12856.

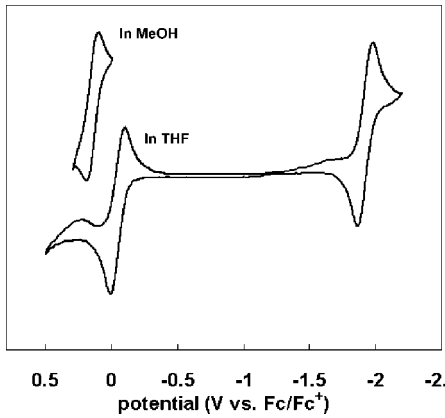

Figure 4. Cyclic voltammogram of 1.0 mM **2a** in THF and MeOH at 25 °C: electrolyte, 0.1 M $[NBu_4][PF_6]$; working electrode, Pt; scan rate, 100 mV/s. Potentials are referenced to Fc/Fc^+.

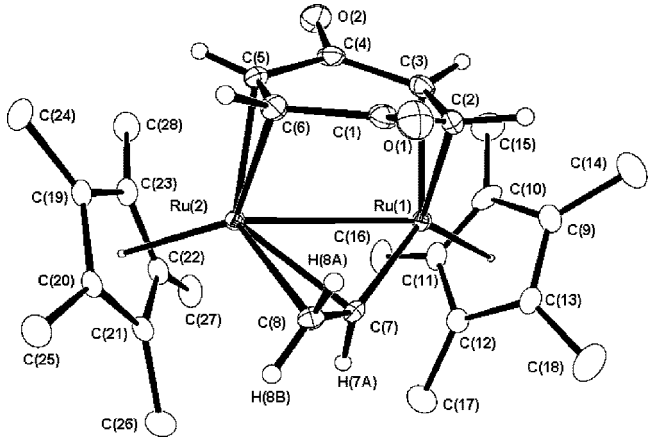

Figure 5. Molecular structure and labeling scheme of **3** with thermal ellipsoids at the 30% probability level.

rates were considerably different. Conversion of **2a** was only 40% for 190 h in benzene-d_6, whereas it reached 90% for the same period in methanol-d_4. The rate constant k was obtained by assuming that the reaction was a pseudo-first-order reaction upon the concentration of **2a**, and the rate constant k was estimated at $(2.7 \pm 0.2) \times 10^{-3}$ s^{-1} in benzene, whereas it was $(10.8 \pm 1.0) \times 10^{-3}$ s^{-1} in methanol.

In the ^1H NMR spectrum of **3**, three coupled signals were found at δ 4.32 (d, $J_{H-H} = 10.0$ Hz), 4.36 (d, $J_{H-H} = 14.0$ Hz), and 7.49 (dd, $J_{H-H} = 14.0$ and 10.0 Hz). This clearly showed the formation of a μ-η^2-vinyl group. Consequently, two inequivalent signals derived from the two Cp* appeared at δ 1.69 and 1.73.

An X-ray diffraction study was carried out using an orange single crystal of **3** obtained from the THF solution. There were two independent molecules, which have similar structural parameters, in the unit cell. The structure of one molecule is depicted in Figure 5, and relevant bond lengths and angles are listed in Table 3. The ORTEP diagram clearly showed the formation of a vinyl group, which was σ-bonded to Ru(1) and π-bonded to Ru(2).

The Ru(1)−Ru(2) distance (2.9104(3) Å) increased by the formation a μ-vinyl group; this distance was greater than that in **2a**, and it was within the range of a Ru−Ru single bond distance. Due to steric repulsion, two Cp* groups moved away from the μ-vinyl group with respect to the Ru−Ru vector. Other structural parameters of **3**, particularly those around the benzoquinone moiety, were similar to those of **2a**.

Fluxional behavior due to the oscillation of a bridging vinyl group has been occasionally reported for μ-vinyl complexes (Scheme 1).[18] As other precedents, fluxional behavior stemming from this motion is also observed in **3**. The ^1H NMR spectrum reached a low temperature limit at −60 °C. The shapes of the signals derived form the Cp* groups and the methine protons on the benzoquinone ligand became broad and coalesced into one signal with an increase in temperature (Figure 6), while the shapes of the other signals that originated from the hydride and the vinyl group did not change.

The hydrogen bond at the oxygen atom of the benzoquinone ligand also affects this fluxional process. The vinyl group moves faster in methanol-d_4 than in toluene-d_8. The rate of the fluxional process in methanol-d_4 was estimated to be 320 s^{-1} at −20 °C on the basis of line shape analysis, while in toluene-d_8, it was estimated to be 65.0 s^{-1} at the same temperature.

The activation parameters of this process were obtained from the VT-NMR studies, ranging from −60 to 20 °C. The enthalpy of activation, $\Delta H^{\ddagger}$, and the entropy of activation, $\Delta S^{\ddagger}$, in methnol-d_4 were estimated to be 14.0 ± 0.4 kcal mol^{-1} and -8.4 ± 2 cal mol^{-1} K^{-1}, respectively. In the VT-NMR studies conducted in toluene-d_8, these values were different: $\Delta H^{\ddagger} = 12.4 \pm 0.4$ kcal mol^{-1}, $\Delta S^{\ddagger} = -0.9 \pm 2$ cal mol^{-1} K^{-1}. These differences strongly imply that the presence of a hydrogen bond affects the transition state of the fluxional process. The acceleration of the oscillation of the vinyl group in a protic solvent is also rationalized by a decrease in the electron density at the metal center. Since the hydrogen bond in benzoquinone causes electron transfer from the metal center to the benzoquinone ligand, the back-donation to the vinyl group is reduced. Thus, the vinyl group can oscillate between the metal centers more easily.

Conclusion

In summary, we showed the presence of a hydrogen bond between the μ-η^2:η^2-benzoquinone ligand and an alcohol in solution as well as in its crystalline form and also demonstrated that such subtle interactions significantly influence the transition metal center. This was estimated by means of UV−vis, IR, and NMR spectroscopy, cyclic voltammogram, and X-ray diffraction studies. A hydrogen bond through a redox-active benzoquinone ligand induces electron transfer from a metal center to the ligand. This electron transfer influences the acidity of the metal center.

Since complex **2** has a hydrido ligand, the effect of the hydrogen bond on the benzoquinone ligand can be assessed by the reactivity of **2**. The reaction of **2a** with acetylene, which afforded a μ-vinyl complex **3**, was significantly accelerated in a protic solvent. The reaction rate in methanol was 3 times faster that in benzene. We are now focusing on the chemical oxidation and reduction of the μ-benzoquinone complex to isolate the one-electron-oxidized and -reduced species as well as protonation using a strong acid.

Experimental Section

General Procedures. All experiments were carried out under an argon atmosphere. All compounds were treated with Schlenk techniques. Dehydrated tetrahydrofuran, toluene, pentane, and

(18) (a) Keister, J. B.; Shapley, J. R. *J. Organomet. Chem.* **1975**, *85*, C29–C31. (b) Shapley, J. R.; Richters, S. I.; Tachikawa, M.; Keister, J. B. *J. Organomet. Chem.* **1975**, *94*, C43–C46. (c) Clauss, A. D.; Tachikawa, M.; Shapley, J. R.; Pierpont, C. G. *Inorg. Chem.* **1981**, *20*, 1528–1533. (d) Koike, M.; Hamilton, D. H.; Wilson, S. R.; Shapley, J. R. *Organometallics* **1996**, *15*, 4930–4938.

Table 3. Selected Bond Lengths (Å) and Angles (deg) of 3

Ru(1)−Ru(2)	2.9103(3)	Ru(1)−C(2)	2.180(3)	Ru(1)−C(3)	2.123(3)
Ru(1)−C(7)	2.055(3)	Ru(2)−C(5)	2.160(3)	Ru(2)−C(6)	2.180(3)
Ru(2)−C(7)	2.196(3)	Ru(2)−C(8)	2.297(3)	C(1)−O(1)	1.234(4)
C(1)−C(2)	1.464(4)	C(1)−C(6)	1.472(4)	C(2)−C(3)	1.435(4)
C(3)−C(4)	1.465(4)	C(4)−O(2)	1.234(4)	C(4)−C(5)	1.483(4)
C(5)−C(6)	1.422(4)	C(7)−C(8)	1.387(4)		
C(7)−Ru(1)−Ru(2)	48.85(8)		C(2)−Ru(1)−C(3)	38.94(12)	
C(5)−Ru(2)−C(6)	38.25(11)		C(7)−Ru(2)−Ru(1)	44.82(7)	
C(7)−Ru(2)−C(8)	35.88(11)		O(1)−C(1)−C(2)	122.5(3)	
O(1)−C(1)−C(6)	120.8(3)		C(2)−C(1)−C(6)	116.7(3)	
C(1)−C(2)−C(3)	119.3(3)		C(2)−C(3)−C(4)	121.5(3)	
O(2)−C(4)−C(3)	123.1(3)		O(2)−C(4)−C(5)	121.1(3)	
C(3)−C(4)−C(5)	115.9(3)		C(4)−C(5)−C(6)	120.8(3)	
C(1)−C(6)−C(5)	120.2(3)				
Ru(3)−Ru(4)	2.9165(3)	Ru(3)−C(30)	2.200(3)	Ru(3)−C(31)	2.122(3)
Ru(3)−C(35)	2.049(3)	Ru(4)−C(33)	2.146(3)	Ru(4)−C(34)	2.190(3)
Ru(4)−C(35)	2.206(3)	Ru(4)−C(36)	2.305(3)	C(29)−O(3)	1.248(4)
C(29)−C(30)	1.454(4)	C(29)−C(34)	1.464(4)	C(30)−C(31)	1.436(5)
C(31)−C(32)	1.465(5)	C(32)−O(4)	1.239(4)	C(32)−C(33)	1.474(5)
C(33)−C(34)	1.422(4)	C(35)−C(36)	1.387(4)		
C(35)−Ru(3)−Ru(4)	49.03(9)		C(30)−Ru(3)−C(31)	38.76(13)	
C(33)−Ru(4)−Ru(34)	38.28(13)		C(35)−Ru(4)−Ru(3)	44.51(8)	
C(35)−Ru(4)−C(36)	35.75(12)		O(3)−C(29)−C(30)	122.2(3)	
O(3)−C(29)−C(34)	119.9(3)		C(30)−C(29)−C(34)	117.9(3)	
C(29)−C(30)−C(31)	118.9(3)		C(30)−C(31)−C(32)	121.3(3)	
O(4)−C(32)−C(31)	122.1(3)		O(4)−C(32)−C(33)	121.0(3)	
C(31)−C(32)−C(33)	116.8(3)		C(32)-C33)-C(34)	120.9(3)	
C(29)−C(34)−C(33)	119.7(3)				

Scheme 1. Oscillation of the μ-Vinyl Group in 3

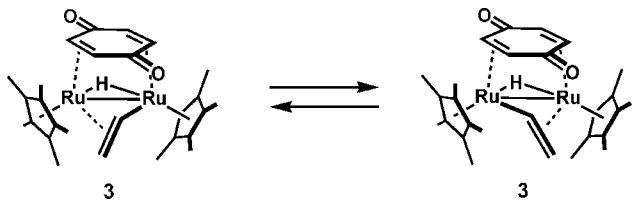

methanol used in this study were purchased from Kanto Chemicals and stored under an argon atmosphere. Benzene-d_6 and toluene-d_8 were dried over sodium-benzophenone ketyl and stored under an argon atmosphere. Trifluoroethanol, hexafluoro-2-propanol, 2-propanol, and methanol-d_4 were degassed and stored under an argon atmosphere. Other materials used in this research were used as purchased. IR spectra were recorded on a JASCO FT/IR-4200 spectrophotometer. UV−vis spectra were recorded on a Shimadzu UV-2550 spectrophotometer. ^{1}H and ^{13}C NMR spectra were recorded on a Varian INOVA-400 spectrometer with tetramethylsilane as an internal standard. Elemental analyses were performed on a Perkin-Elmer 2400 series CHN analyzer. Cyclic voltammograms were performed using a BAS CV-50W voltammetric analyzer interfaced to a personal computer. The working electrode was platinum, and the counter electrode was a platinum wire. The reference electrode was a silver wire housed in a glass tube sealed with a porous Vycor tip and filled with a 0.1 M solution of $AgNO_3$ in acetonitrile. The data obtained as relative to a reference electrode (Ag/Ag^+) were converted to the potential relative to the redox potential of ferrocene, which was measured under the same conditions at the same time. Tetrabutylammonium hexafluorophosphate ($TBAPF_6$) (Wako) was recrystallized from THF, dried under vacuum, and stored under an argon atmosphere. A rotating disk electrode experiment was carried out on a Hokuto-Denko HSV-100 voltammetric analyzer using Metrohm 628−10 rotating disk electrode assemblies under the same conditions as the CV analyses.

X-ray Structure Determination. X-ray-quality crystals of **2a**, **2a-PhOH**, and **3** were obtained from the preparations described below and mounted on nylon Cryoloops with Paratone-N (Hampton Research Corp.). Diffraction experiments of **2a**, **2a-POH**, and **3** were performed on a Rigaku RAXIS-RAPID imaging plate with graphite-monochromated Mo Kα radiation ($\lambda = 0.71069$ Å). Cell refinement and data reduction were performed using the PROCESS-AUTO program.[19] Intensity data were corrected for Lorentz−polarization effects and for empirical and numerical absorption. The structure of **2a** was solved by a Patterson method and subsequent Fourier difference techniques. The structures of **2a-POH** and **3** were solved by a direct method and subsequent Fourier difference techniques. The structures were refined anisotropically for all non-hydrogen atoms by full-matrix least-squares calculation on F^2 using the SHELX-97 program package.[20] All hydrogen atoms were refined isotropically. Neutral atom scattering factors were obtained from the standard sources.[21] The metal-bound hydrogen atoms of **2a** and **2a-PhOH** and two hydrogen atoms bound to the benzoquinone ligand of **2a-PhOH** were located in a difference Fourier map and refined isotropically. Crystal data and results of the analyses are listed in Table 4.

Variable-Temperature NMR Spectra and Dynamic NMR Simulations. Variable-temperature NMR studies were performed in flame-sealed NMR tubes in toluene-d_8 and methanol-d_4 for **2a** using a Varian INOVA-400 Fourier transform spectrometer. NMR simulations for the methine proton on the benzoquinone ligand and Cp* signals of **2a** were performed using gNMR v4.1.0. (1995−1999 Ivory Soft). Final simulated line shapes were obtained via an iterative parameter search upon the exchange constant k. Full details of the fitting procedure are shown in the Supporting Information. The rate constants that accurately modeled the experimental spectra at selected temperature are also given in the Supporting Information.

(19) *PROCESS-AUTO*, Automatic Data Acquisition and Processing Package for Imaging Plate Diffractometer; Rigaku Corporation: Tokyo (Japan), 1998.

(20) Sheldrick, G. M. *SHELX-97*, Program for Crystal Structure Determination; University of Göttingen: Göttingen (Germany), 1997.

(21) *International Tables for X-ray Crystallography*; Kynoch Press: Birmingham, U.K., 1975; Vol. 4.

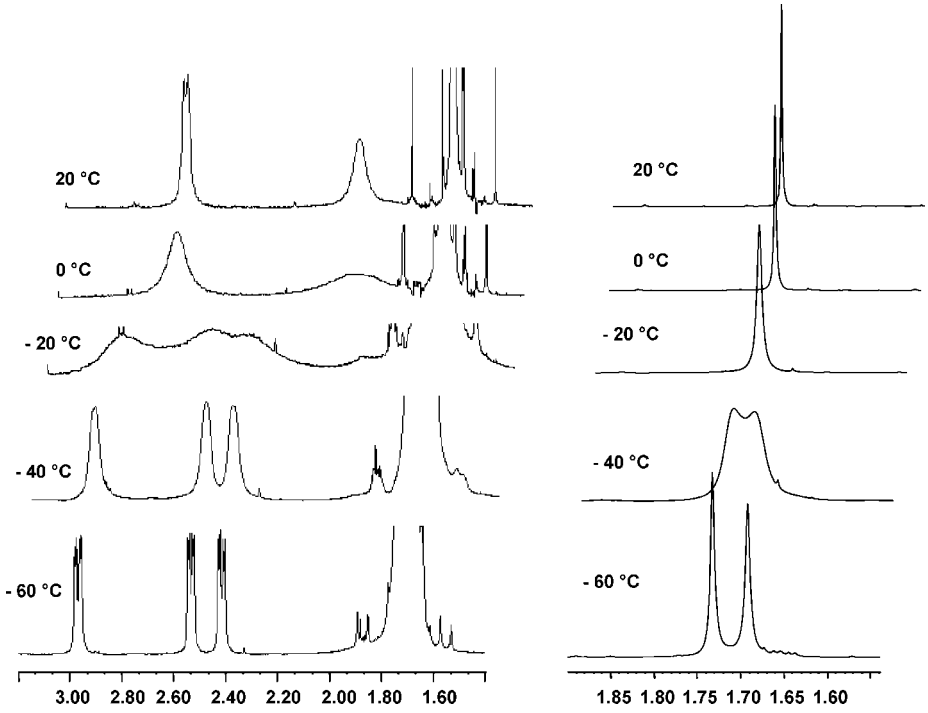

Figure 6. VT-NMR spectra of **3** in methanol-d_4 showing the signals for the methine protons on the benzoquinone ligand (left) and the signals for the Cp* groups (right). One of the four methine protons was obscured by the signals of the Cp* group (δ 1.69 and 1.73 at −60 °C) below 0 °C.

Table 4. Crystallographic Data for 2a, 2a-PhOH, and 3

	2a	2a-PhOH	3
(a) Crystal Data			
empirical formula	$C_{26}H_{36}O_2Ru_2$	$C_{26}H_{36}O_3Ru_2 \cdot (C_6H_6O)_{2.5}$	$C_{28}H_{38}O_2Ru_2$
fw	582.69	817.96	608.72
cryst description	block	platelet	block
cryst color	dark green	red	red
cryst size (mm)	0.50 × 0.20 × 0.10	0.35 × 0.30 × 0.10	0.50 × 0.18 × 0.14
crystallizing solution	THF/pentane (25 °C)	THF/pentane (25 °C)	THF/toluene (25 °C)
cryst syst	monoclinic	monoclinic	monoclinic
space group	*C2/c* (#15)	$P2_1/n$ (#14)	$P2_1/a$ (#14)
lattice params	a = 18.3466(7) Å	a = 8.64090(16) Å	a = 17.6283(5) Å
	b = 8.7694(3) Å	b = 33.7320(6) Å	b = 14.9024(4) Å
	c = 30.5284(10) Å	c = 13.1044(3) Å	c = 20.4564(7) Å
	β = 103.4840(11)°	β = 103.5980(7)°	β = 113.0420(11)°
V (Å^3)	4776.3(3)	3712.54(12)	4945.2(2)
Z value	8	4	8
D_{calc} (g/cm^3)	1.621	1.476	1.635
measurement temp (°C)	−80	−80	−120
μ(Mo Kα) (mm^{-1})	1.284	0.856	1.244
(b) Intensity Measurements			
diffractometer	RAXIS-RAPID	RAXIS-RAPID	RAXIS-RAPID
radiation	Mo Kα	Mo Kα	Mo Kα
monochromator	graphite	graphite	graphite
2θ max (deg)	60	60	55
no. of reflns collected	23 560	60 471	42 498
no. of indep reflns	5818 (R_{int} = 0.0280)	8647 (R_{int} = 0.0214)	11 667 (R_{int} = 0.0300)
no. of reflns obsd (>2σ)	4988	7765	9782
abs correction type	empirical	empirical	numerical
abs transmn	0.7944 (min.),	0.8747 (min.),	0.7758 (min.),
	1.0000 (max.)	1.0000 (max.)	0.9129 (max.)
(c) Refinement (Shelxl-97-2)			
R_1 (I > 2σ(I))	0.0204	0.0192	0.0333
wR_2 (I > 2σ(I))	0.0504	0.0493	0.0666
R_1 (all data)	0.0234	0.0217	0.0402
wR_2 (all data)	0.0518	0.0507	0.0689
no. of data/restraints/params	5455/0/305	8463/0/517	11 219/0/634
GOF	1.080	1.056	1.103
largest diff peak and hole (e Å^{-3})	0.643 and −0.310	0.378 and −0.354	2.167 and −0.619

The activation parameters, $\Delta H^{\ddagger}$ and $\Delta S^{\ddagger}$, were determined from the plot of ln(k/T) versus 1/T. Estimated standard deviations (σ) in the slope and y-intercept of the Eyring plot determined the error in $\Delta H^{\ddagger}$ and $\Delta S^{\ddagger}$, respectively. The standard deviation in $\Delta G^{\ddagger}$ was

determined from the formula $\sigma(\Delta G^{\ddagger})^2 = \sigma(\Delta H^{\ddagger})^2 + [T\sigma(\Delta S^{\ddagger})]^2 - 2T\sigma(\Delta H^{\ddagger})\,\sigma(\Delta S^{\ddagger})$.

Preparation of the μ-η^2:η^2-Benzoquinone Complex {Cp*Ru(μ-H)}$_2$(μ-η^2:η^2-$C_6H_4O_2$) (2a). Toluene (5 mL) and diruthenium tetrahydrido complex **1** (0.366 g, 0.768 mmol) were charged in a reaction flask. A 1.1 equiv amount of 1,4-benzoquinone (94.3 mg, 0.872 mmol) was added to the solution at 25 °C. The solution was vigorously stirred for 2 h at 25 °C. The color of the solution changed from red to light brown. After the solvent was removed under reduced pressure, the residual solid was dissolved in 2 mL of THF. In order to remove the remaining 1,4-benzoquinone, the residual solid was then purified by the use of column chromatography on alumina (Merck, Art. No. 1097) with THF. Removal of the solvent under reduced pressure afforded a 0.421 g amount of **2a** as a brownish-green solid (94% yield). A single crystal used for the diffraction studies was prepared by the slow diffusion of pentane to the THF solution of **2a** at room temperature. ^{1}H NMR (400 MHz, 23 °C, benzene-d_6): δ −16.26 (s, 2H, Ru*H*), 1.30 (s, 30H, C_5Me_5), 5.27 (s, 4H, $C_6H_4O_2$). ^{1}H NMR (400 MHz, 23 °C, methanol-d_4): δ −15.73 (s, 2H, Ru*H*), 1.71 (s, 30H, C_5Me_5), 5.18 (s, 4H, $C_6H_4O_2$). ^{13}C NMR (100 MHz, 23 °C, benzene-d_6): δ 9.8 (q, J_{C-H} = 126 Hz, C_5Me_5), 72.0 (d, J_{C-H} = 161 Hz, $C_4H_4(CO)_2$), 93.4 (s, C_5Me_5), 189.5 (s, *C*O). ^{13}C NMR (100 MHz, 23 °C, methanol-d_4): δ 10.2 (q, J_{C-H} = 127 Hz, C_5Me_5), 70.3 (d, J_{C-H} = 163 Hz, $C_6H_4O_2$), 97.4 (s, C_5Me_5), 190.9 (s, *C*O). IR (KBr): 704, 881, 945, 1023, 1116, 1283, 1375, 1458, 1619 (νCO), 2906, 3004 (cm^{-1}). Anal. Calcd for $C_{26}H_{36}O_2Ru_2$: C, 53.59; H, 6.23. Found: C, 53.23; H, 6.20.

Preparation of the μ-η^2:η^2-2-Methylbenzoquinone Complex {Cp*Ru(μ-H)}$_2$(μ-η^2:η^2-$C_6MeH_3O_2$) (2b). Toluene (5 mL) and diruthenium tetrahydrido complex **1** (0.315 g, 0.661 mmol) were charged in a reaction flask. A 1.2 equiv amount of 2-methyl-1,4-benzoquinone (97.6 mg, 0.799 mmol) was added to the solution at 25 °C. The solution was vigorously stirred for 3 h at 25 °C. The color of the solution changed from red to reddish-purple. After the solvent was removed under reduced pressure, the residual solid was dissolved in 2 mL of THF. In order to remove the remaining 2-methyl-1,4-benzoquinone, the residual solid was then purified by the use of column chromatography on alumina (Merck, Art. No. 1097) with THF. Removal of the solvent under reduced pressure afforded a 0.173 g amount of **2b** as a reddish-purple solid (44% yield). ^{1}H NMR (400 MHz, 23 °C, benzene-d_6): δ −16.88 (d, J_{H-H} = 4.4 Hz, 1H, Ru*H*), −16.22 (d, J_{H-H} = 4.4 Hz, 1H, Ru*H*), 1.32_6 (s, 15H, C_5Me_5), 1.33_3 (s, 15H, C_5Me_5), 1.83 (s, 3H, $C_6MeH_3O_2$), 5.04 (dd, J_{H-H} = 7.2, 3.0 Hz, $C_6MeH_3O_2$), 5.41 (d, J_{H-H} = 7.2 Hz, $C_6MeH_3O_2$), 5.91 (d, J_{H-H} = 3.0 Hz, $C_6MeH_3O_2$). ^{13}C NMR (100 MHz, 23 °C, benzene-d_6): δ 9.9 (q, J_{C-H} = 127 Hz, C_5Me_5), 10.6 (q, J_{C-H} = 127 Hz, C_5Me_5), 23.3 (q, J_{C-H} = 127 Hz, $C_6MeH_3O_2$), 71.1 (d, J_{C-H} = 158 Hz, $C_4MeH_3(C{=}O)_2$), 72.3 (d, J_{C-H} = 159 Hz, $C_4MeH_3(C{=}O)_2$), 81.9 (s, $C_4MeH_3(C{=}O)_2$), 82.2 (d, J_{C-H} = 157 Hz, $C_4MeH_3(C{=}O)_2$), 93.1 (s, C_5Me_5), 93.5 (s, C_5Me_5), 186.6 (s, *C*O), 188.0 (s, *C*O). IR (KBr): 711, 871, 944 1025, 1095, 1265, 1380, 1461, 1618 (νCO), 2906, 2961, 2993 (cm^{-1}). Anal. Calcd for $C_{27}H_{38}O_2Ru_2$: C, 54.35; H, 6.42. Found C, 54.32; H, 6.66.

Preparation of the Phenol Adduct of a μ-η^2:η^2-Benzoquinone Complex, {Cp*Ru(μ-H)}$_2$(μ-η^2:η^2-$C_6H_4O_2$)·(PhOH)$_{2.5}$ (2a-PhOH). Complex **2a** (9.5 mg, 16 μmol) and phenol (157.0 mg, 1.67 mmol) were dissolved in THF (0.5 mL) and divided into two microtubes. These microtubes were put in 50 mL Schlenk tubes with 8 mL of pentane. Orange needlelike crystals of the phenol adduct were obtained by standing the flask for 5 days at 25 °C. The crystals were separated by decantation and rinsed three times with 2 mL of pentane. A 4.5 mg amount of the phenol adduct **2a-PhOH** was obtained by drying under reduced pressure (34% yield). IR (KBr): 693, 710, 756, 816, 879, 1024, 1070, 1099, 1119, 1166, 1233, 1249, 1271, 1330, 1376, 1473, 1499, 1568 (νCO), 1596, 3072 (νOH) (cm^{-1}). Anal. Calcd for $C_{26}H_{36}O_2Ru_2\cdot(PhOH)_{2.5}$: C, 60.20; H, 6.28. Found: C, 60.03; H, 6.49.

Preparation of the μ-η^2-Vinyl-μ-η^2:η^2-benzoquinone Complex (Cp*Ru)$_2$(μ-H)(μ-η^2-CH=CH$_2$)(μ-η^2:η^2-$C_6H_4O_2$) (3). Methanol (3 mL) and μ-η^2:η^2-benzoquinone complex **2a** (53.2 mg, 91.3 μmol) were charged in a flask. After the solution was frozen in a liquid nitrogen bath, the reaction flask was degassed by the use of a vacuum line. Then, 1 atm of acetylene was introduced into the reaction flask at 25 °C. The solution was vigorously stirred for 13 days at 25 °C. The color of the solution changed from light green to red. After the solvent was removed under reduced pressure, the residual solid was dissolved in 2 mL of THF. The residual solid was then purified by the use of column chromatography on alumina (Merck, Art. No. 1097) with THF. Removal of the solvent under reduced pressure afforded a 52.5 mg amount of **3** as an orange solid (94% yield). A single crystal used for the diffraction studies was prepared from a THF solution of **3** by slow evaporation at room temperature. ^{1}H NMR (400 MHz, −60 °C, methanol-d_4): δ −19.82 (s, 1H, Ru*H*), 1.65 (dd, J_{H-H} = 6.8, 3.0 Hz, 1H, $C_6H_4O_2$), 1.69 (s, 15H, C_5Me_5), 1.73 (s, 15H, C_5Me_5), 2.41 (dd, J_{H-H} = 7.6, 3.0 Hz, 1H, $C_6H_4O_2$), 2.53 (dd, J_{H-H} = 6.8, 3.2 Hz, 1H, $C_6H_4O_2$), 2.97 (dd, J_{H-H} = 7.6, 3.2 Hz, 1H, $C_6H_4O_2$), 4.32 (d, J_{H-H} = 10.0 Hz, 1H, −CH=C*H*H), 4.36 (d, J_{H-H} = 14.0 Hz, 1H, −CH=CH*H*), 7.49 (dd, J_{H-H} = 14.0, 10.0 Hz, 1H, −C*H*=CHH). ^{13}C{^{1}H} NMR (100 MHz, −60 °C, methanol-d_4): δ 9.6 (C_5Me_5), 10.4 (C_5Me_5), 48.7 ($C_4H_4(CO)_2$), 52.3 ($C_4H_4(CO)_2$), 55.2 ($C_4H_4(CO)_2$), 55.4 ($C_4H_4(CO)_2$), 75.8 (−CH=*C*H$_2$), 97.9 (C_5Me_5), 98.3 (C_5Me_5), 148.5 (−*C*=CH$_2$), 205.4 (*C*O), 213.6 (*C*O). IR (ATR): 639, 654, 799, 1020, 1092, 1261, 1291, 1380, 1621 (νCO) (cm^{-1}). Anal. Calcd for $C_{28}H_{38}O_2Ru_2$: C, 55.25; H, 6.29. Found: C, 55.13; H, 6.45.

Kinetic Experiments of the Reaction of 2a with Acetylene. Complex **2a** (3.5 mg, 6 μmol) and hexamethylbenzene (1.3 mg, 8 μmol) as an internal standard were dissolved in toluene (3 mL). The solution was divided into two equal parts and charged in an NMR tube equipped with a Teflon valve. After the solvent was removed in vacuo, 0.5 mL of benzene-d_6 was added to one of the two NMR tubes and 0.5 mL of methanol-d_4 to the other to dissolve the resulting solid. After the solution was frozen in a liquid nitrogen bath, each NMR tube was degassed by the use of a vacuum line. Then, 1 atm of acetylene was introduced into each NMR tube at 25 °C. After the NMR tubes were sealed, each solution was allowed to react at 25 °C. The consumption of **2a** was monitored by means of ^{1}H NMR spectroscopy, and the intensities of the resonance of the hydrido ligand were recorded periodically. At regular times, the distribution of **2a** was estimated by dividing the integral value for **2a** by the integral values for hexamethylbenzene. This value was used for the determination of the rate constant. The rate constants obtained at each solvent were as follows: $k_{benzene}$ = (2.7 ± 0.2) × 10^{-3} s^{-1} and k_{MeOH} = (10.8 ± 1.0) × 10^{-3} s^{-1}.

Acknowledgment. This work is supported by Grants No. 18105002 (Scientific Research (S)) and No. 19550058 (Scientific Research (C)) from Japan Society of the Promotion of Science. This work was partly supported by the global COE program of the Japan Society for the Promotion of Science.

Supporting Information Available: Results of the X-ray diffraction studies and crystallographic files of **2a**, **2a-POH**, and **3**; the X-ray data are also given as CIF files. Results of the dynamic NMR studies of **3**, UV−vis spectra of **2a** and **2b**, and CV analyses of **2a** and **2b**. These materials are available free of charge via the Internet at http://pubs.acs.org.

OM800363F